Kinetic Study on Reactions of 1- and 2-Methylvinoxy Radicals with O_2

Tatsuo Oguchi, Akira Miyoshi,* Mitsuo Koshi, Hiroyuki Matsui, and Nobuaki Washida

Department of Chemical System Engineering, The University of Tokyo, 7-3-1 Hongo, Bunkyo-ku, Tokyo 113-8656, Japan, and The National Institute for Environmental Studies, 16-2 Onogawa, Tsukuba-shi, Ibaraki, 305-0053, Japan

Received: May 18, 2000; In Final Form: October 12, 2000

The reactions of 1- and 2-methylvinoxy radicals with O_2 have been studied by laser-induced fluorescence coupled with pulsed laser photolysis of precursor molecules at room temperature (298 ± 5 K). The rate constants for both reactions showed typical falloff pressure dependence in the investigated pressure range (8−330 Torr, He buffer), which suggests the dominance of recombination processes to form peroxy radicals. From the Rice−Ramsperger−Kassel−Morcus fit to the experimental data, the limiting high-pressure rate constants were derived to be k^{∞} (1-methylvinoxy + O_2) = 9.8×10^{-13} and k^{∞} (2-methylvinoxy + O_2) = 1.3×10^{-12} cm^3 molecule^{-1} s^{-1}, which are 5−7 times larger than that for the reaction of a nonsubstituted vinoxy radical. The influence of the methyl substituent effect and the resonance stabilization on the rate constants is discussed.

Introduction

The vinoxy radical (CH_2CHO) is the simplest alkenoxy radical that is produced in the reaction of O(^{3}P) with ethylene. By using the laser-induced fluorescence (LIF) spectrum, which was first observed by Inoue and Akimoto,[1] several kinetic studies on the reactions with O_2,[2,3] NO,[2] and NO_2[4] have been reported in the last two decades. Also, cavity ring-down spectroscopic studies on the reaction with O_2 have been carried out by Zhu and Johnston,[5] who reported the pressure dependence of the rate constants in the wide range of pressure. The CH_2CHO radical is thought to have a resonance electronic structure between the two localized states, "ethenyloxy" and "formylmethyl" radicals, although ab initio theoretical calculations[6,7] and a microwave spectroscopic study[8] suggested the enhanced character of a carbon-centered radical.

Alkyl-substituted vinoxy radicals are important intermediates because they are produced in the reactions of O(^{3}P) with higher alkenes,[9] hydrogen-atom abstraction reactions from ketones and aldehydes,[9] or the reactions of OH radicals with alkynes.[10] However, little is known for the reactions of these radicals as well as their electronic structures. Recently, Weisshaar and co-workers,[11] Washida et al.,[9] and Bersohn and co-workers[12] reported the LIF spectra for methyl-substituted vinoxy radicals in the similar wavelength region to the vinoxy radical. The observation suggests the similarity of the electronic structure to the vinoxy radical, but slightly enhanced oxy radical character for α-methyl-substituted radicals from the red shift of the band origin.[9]

In the present work, the reactions of 1-methylvinoxy (CH_2COCH_3) and 2-methylvinoxy (CH_3CHCHO) radicals with O_2 have been investigated by the LIF method at room temperature, in the pressure range of 3−330 Torr (1 Torr. ≈ 133.322 Pa) in He buffer. The results were analyzed by a Rice−Ramsperger−Kassel−Marcus calculation. The methyl substituent effect and the resonance stabilization effect on the reactivity are discussed.

* Author for correspondence.

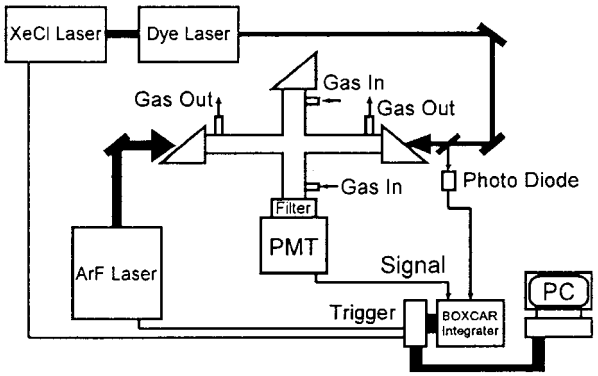

Figure 1. Schematic of the experimental apparatus.

Experimental Section

Experiments were carried out by the LIF technique coupled with pulsed laser photolysis in a slow flow reactor, which is similar to that used in the previous report.[13] A schematic of the apparatus is shown in Figure 1.

The methylvinoxy radicals were generated by the pulsed ArF (193 nm) excimer laser (Lambda Physik LEXTRA50) photolysis of alkenyl alkyl ethers,[9,11]

$$CH_2{=}C(CH_3){-}O{-}CH_3 + h\nu \rightarrow CH_2COCH_3\ (1\text{-methylvinoxy}) + CH_3 \quad (1)$$

$$CH_3CH{=}CH{-}O{-}C_2H_5 + h\nu \rightarrow CH_3CHCHO\ (2\text{-methylvinoxy}) + C_2H_5 \quad (2)$$

The observed fluorescence excitation spectra of 1- and 2-methylvinoxy radicals well matched with the previous observations in bulk condition,[9] and are also in agreement with those in jet-cooled condition.[11] In the kinetic experiments, the methylvinoxy radicals were detected by exciting the $\tilde{B}-\tilde{X}$ transitions[9,11] at 340.6 nm for 1-methylvinoxy and at 340.5 nm for 2-methylvinoxy radicals. The probe light was generated by a dye laser (Lambda Physik LPD3002, *p*-terphenyl) pumped

10.1021/jp001826q CCC: $20.00
Published on Web 12/22/2000

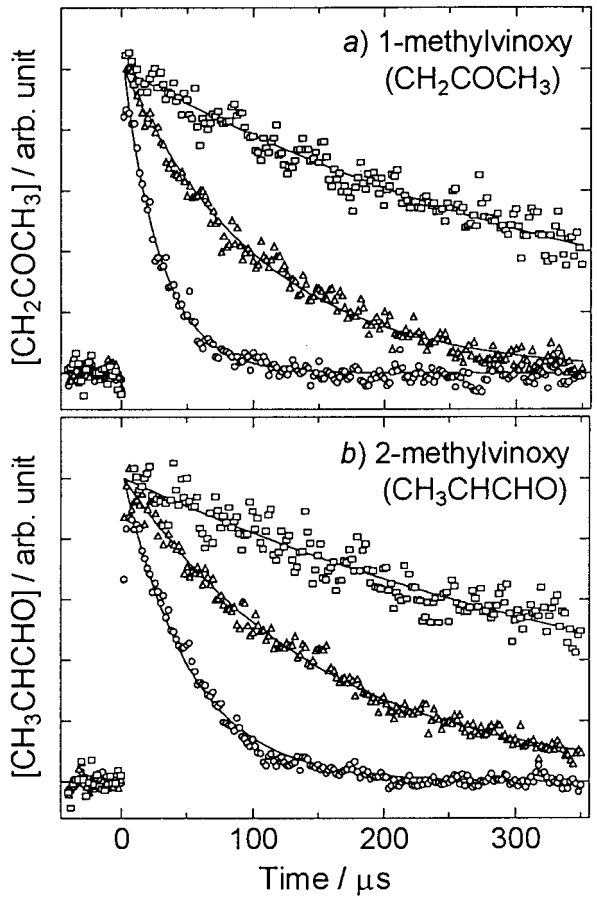

Figure 2. Typical decay profiles of (a) 1-methylvinoxy (CH_2COCH_3) and (b) 2-methylvinoxy (CH_3CHCHO) radicals. Solid lines denote results of single-exponential fitting. Experimental conditions: (a) Total pressure = 333 Torr. □, without O_2; △, $[O_2] = 7.5 \times 10^{15}$ molecules cm^{-3}; ○, $[O_2] = 3.9 \times 10^{16}$ molecules cm^{-3}. (b) Total pressure = 92.7 Torr. □, without O_2; △, $[O_2] = 4.3 \times 10^{15}$ molecules cm^{-3}; ○, $[O_2] = 1.7 \times 10^{16}$ molecules cm^{-3}.

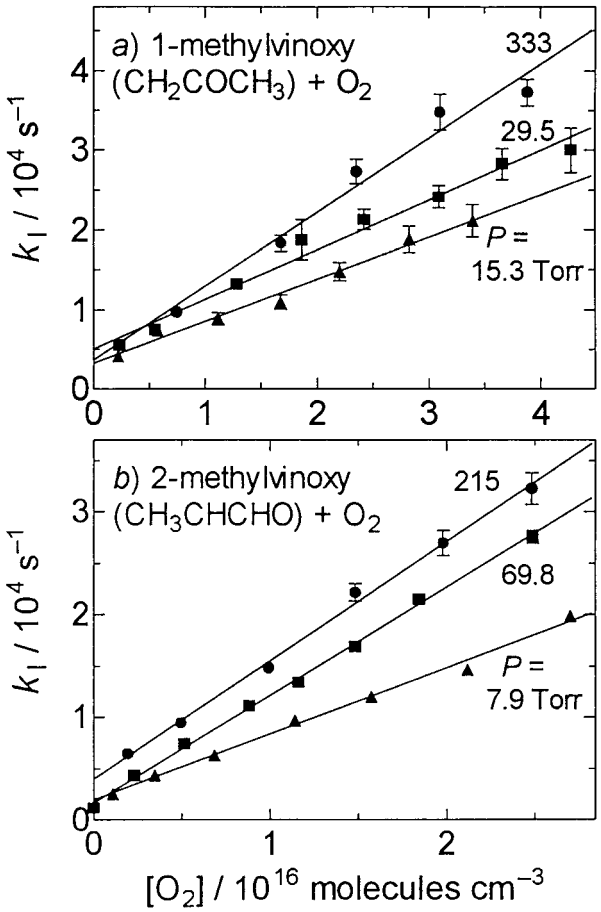

Figure 3. Plots of the first-order decay rate (k_1) of methylvinoxy radicals vs the concentration of O_2. Error bars denote the two standard deviations derived from the least-squares analysis of decay profiles. (a) CH_2COCH_3 (1-methylvinoxy) + O_2. ▲, ■, and ● denote the experiments at total pressures of 15.3, 29.5, and 333 Torr, respectively (He buffer). (b) CH_3CHCHO (2-methylvinoxy) + O_2. ▲, ■, and ● denote the experiments at total pressures of 7.9, 69.8, and 215 Torr, respectively (He buffer).

by a XeCl excimer laser (Lambda Physik LEXTRA200). The fluorescence was detected by a photomultiplier (Hamamatsu R269) through color glass filters (Hoya UV32 and U330; transmit 320−390 nm). The signal from the photomultiplier was amplified and averaged for 10 laser shots by using a boxcar integrator (Stanford Research SR250) and was stored in a personal computer. The time profiles of the radical concentrations were recorded by scanning the delay time between the photolysis and the probe laser pulses.

Gas flows were regulated using mass flow controllers and were premixed before entering the reactor. The linear flow velocity was kept within the range 13−32 cm s^{-1}, at which the gas refresh rate in the cell was ∼1 Hz. The experimental data were obtained at a photolysis rate of 7 Hz, after confirming that no significant difference was found between the results at 1 and 7 Hz (for example, the decay rate of 2-methylvinoxy radical [without O_2] was 1175 ± 89 s^{-1} at 1 Hz and 1240 ± 62 s^{-1} at 7 Hz, under the total pressure of 201 Torr). The total pressures in the reactor were measured using a capacitance manometer (MKS Baratron 122A). He (Nippon Sanso, >99.9999%) was used as a carrier gas. Isopropenyl methyl ether (Tokyo Kasei, 98%) and 1-propenyl ethyl ether (Aldrich, 98%, mixture of cis and trans) were degassed, diluted in He, and stored in a glass reservoir.

The concentration of the precursor in the reactor was around 1.0×10^{14} molecules cm^{-3} ($0.5-4.0 \times 10^{14}$ for 1-methylvinoxy and $0.1-3.2 \times 10^{14}$ for 2-methylvinoxy) and the fluence of the photolysis laser was around 5 mJ cm^{-2}. The concentration of methylvinoxy radicals was estimated to be $(4-20) \times 10^{11}$ molecules cm^{-3} on the basis of the estimated absorption coefficients of precursor ethers. Under these conditions, the effect of side reactions such as radical−radical reaction was negligible for the following reasons: (1) The decay rate of methylvinoxy radicals without O_2 was found to be almost independent of initial concentration of radicals, $[R]_0$. For example, the decay rate of 2-methylvinoxy radical was 1240 s^{-1} at $[R]_0 = 4 \times 10^{11}$ molecules cm^{-3} and 1550 at $[R]_0 = 9 \times 10^{11}$ under 200 Torr of total pressure, and the decay rate of 1-methylvinoxy was 3390 s^{-1} at $[R]_0 = 8 \times 10^{11}$ molecules cm^{-3} and 3290 at $[R]_0 = 2 \times 10^{12}$. (2) Even if the gas kinetic collision rate, 3×10^{-10} cm^3 $molecule^{-1}$ s^{-1}, was assumed for the radical−radical reactions, the upper-limit contribution to the first-order decay rate was estimated to be 100∼500 s^{-1}, whereas the measurements were done under the conditions where the first-order decay rate was typically 10 000−30 000 s^{-1}. All experiments were performed at room temperature (298 ± 5 K).

Results and Discussion

Typical observed decay profiles of 1- and 2-methylvinoxy radicals are shown in Figure 2a and b, respectively. No

TABLE 1: Summary of Experimental Results and Experimental Conditions

total pressure (Torr)	$k \pm 2\sigma$[a] (10^{-13} cm^3 molecule^{-1} s^{-1})	[O_2] range (10^{16} molecules cm^{-3})	[P][b] (10^{14} molecules cm^{-3})
1-methylvinoxy + O_2			
15.3	5.28 ± 0.56	0.2−3.4	3.2
29.5	6.23 ± 0.70	0.2−4.3	3.3
56.1	6.65 ± 0.52	0.4−5.7	4.0
102	7.14 ± 1.02	0.2−4.5	1.0
150	8.44 ± 2.08	0.2−4.7	3.0
164	8.18 ± 1.20	0.4−3.0	0.9
222	8.22 ± 1.36	0.2−5.9	1.0
333	9.27 ± 1.87	0.7−3.9	0.5
2-methylvinoxy + O_2			
7.9	6.42 ± 0.44	0.1−2.7	0.2
14.1	7.96 ± 0.33	0.1−2.5	0.6
19.4	8.52 ± 0.14	0.1−2.3	0.2
30.0	9.24 ± 0.97	0.1−2.6	0.6
51.7	10.70 ± 1.60	0.1−1.9	3.2
69.8	10.51 ± 0.39	0.1−2.5	0.2
92.7	11.73 ± 1.48	0.1−2.5	0.2
107	10.70 ± 1.30	0.1−5.8	1.8
148	10.81 ± 0.72	0.1−3.9	0.9
215	11.60 ± 0.40	0.2−5.7	1.6

[a] Rate constant (k) and its error limit at two standard deviations (2σ). [b] Concentration of the precursor molecule, P, which is $CH_2{=}C(CH_3){-}O{-}CH_3$ for 1-methylvinoxy or $CH_3CH{=}CH{-}O{-}C_2H_5$ for 2-methyl vinoxy.

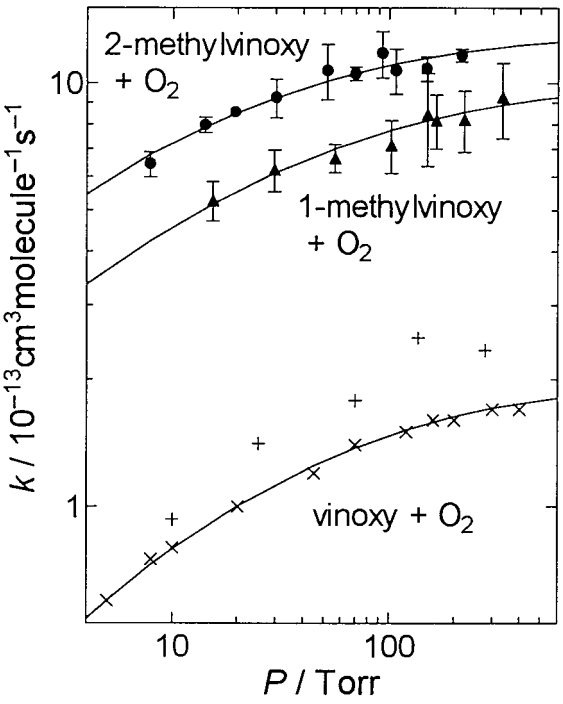

Figure 4. Pressure dependence of the second-order rate constants (k) for CH_2COCH_3 (1-methylvinoxy) + O_2 (▲) and CH_3CHCHO (2-methylvinoxy) + O_2 (●). The rate constants of CH_2CHO (vinoxy) + O_2 are from ref 3 (+) and ref 5 (×). Solid lines denote the best fit results of RRKM calculation. For CH_2CHO + O_2, the RRKM fit was made to the experimental data in ref 5. See text for detail.

significant deviation from the single-exponential decay was observed in either profile obtained with or without O_2. The measured pseudo-first-order decay rates of 1- and 2-methylvinoxy radicals are plotted against O_2 concentrations in Figure 3a and b, respectively. The error bar on each point denotes the error limit at two standard deviations derived from the least-squares analysis. The decay rates linearly depend on [O_2], as shown in Figure 3a and b, and the second-order rate constants were derived from the slopes of the plots.

As can be found in Figure 3a and b, the second-order rate constants for both reactions strongly depend on pressures, whichindicates that the reactions involve the three-body mechanism. Therefore, the measurements were carried out under the pressure range 3−330 Torr with He buffer gas. The experimental results as well as the experimental conditions are summarized in Table 1. To avoid the significant contribution of O_2 as a third body, the fraction of O_2 in the total pressure was limited to below ∼10%. Even in the worst case, P = 7.9 Torr run for 2-methylvinoxy + O_2 shown in Figure 3b, the measured rate constants linearly depend on [O_2] and no apparent quadratic dependence (expected if the third body effect of O_2 is significant) was found.

The results are shown in Figure 4 along with the rate constants for nonsubstituted vinoxy radical + O_2 reported previously.[3,5] The error bars shown in Figure 4 indicate the error limits at two standard deviations derived by least-squares analysis. The solid lines indicate the results of RRKM calculations, which will be described below. The observed pressure dependence shows the typical falloff behavior and suggests the dominance of the recombination processes for 1- and 2-methylvinoxy + O_2 reactions. The high-pressure limiting rate constants for 1- and 2-methylvinoxy radicals are about 5−7 times larger than that for nonsubstituted vinoxy radical.

From the observed falloff behavior, the dominant reaction processes are expected to be the recombination reactions forming peroxy radicals,

$$CH_2COCH_3 + O_2 + M \rightarrow CH_2(OO^{\bullet})COCH_3 + M \quad (3)$$

$$CH_3CHCHO + O_2 + M \rightarrow CH_3CH(OO^{\bullet})CHO + M \quad (4)$$

$$CH_2CHO + O_2 + M \rightarrow CH_2(OO^{\bullet})CHO + M \quad (5)$$

where, it is assumed that the oxygen molecules are attached to the carbon atoms at 2-position because the vinoxy radicals should have a character of the carbon-centered radical.[4,7,8] The formation of the trioxy radical (ROOO•) will not be feasible because of its thermochemical instability.[14]

To verify the recombination mechanism, as well as to extract the limiting high-pressure rate constants, RRKM calculations were performed. The molecular parameters used in the RRKM calculations were estimated at the B3LYP[15]/6-31G(d) level and

TABLE 2: Best-Fit Parameters and Rate Constants Derived by RRKM Calculation

reaction	ΔH_0[a]/kJ mol^{-1}	$E_{0,rec}$ kJ mol^{-1}	$\langle\Delta E_{down}\rangle$/cm^{-1}	k^0 (10^{-29} cm^6 s^{-1})	k^∞ (10^{-13} cm^3 s^{-1})	$[M]_c$[b] (10^{15} cm^{-3})
$CH_2COCH_3 + O_2$	−120.77	−2.50 ± 0.20	24 ± 6	13(2.3)[c]	9.8 ± 0.8	7.7
$CH_3CHCHO + O_2$	−112.69	−3.51 ± 0.18	54 ± 12	25(1.9)[c]	13.0 ± 1.0	5.3
$CH_2CHO + O_2$[d]	−112.34	3.06 ± 0.07	123 ± 8	0.43(1.3)[c]	1.97 ± 0.06	46

[a] Estimated by G2 method. [b] Falloff density defined as k^∞/k^0. [c] Values in parentheses are uncertainty factors at two standard deviations. [d] Best fit was performed to experimental data in ref 5.

the heats of reaction were estimated by the G2 method.[16] All the calculations were performed by using the *Gaussian 98* program.[17] Some torsion vibrations were treated as hindered rotors.[18] The estimated molecular parameters were summarized in Tables 1S−5S. The effects of the variational transition states treatment was found to be minor (see Figure 1S for detail) and was not taken into account. Although the effect was minor, the angular momentum conservation was included by evaluating the *J*-averaged microcanonical rate constants.[19] The steady-state solution to the master equation was obtained by using *UNIMOL Program Suite*.[20] The threshold energy, E_0, and the average downward energy transferred per collision, $\langle\Delta E_{down}\rangle$, were adjusted so as to reproduce the experimental results.

The best-fit results are shown in Figure 4 by solid lines, and the derived parameters are shown in Table 2. The limiting high-pressure rate constants (k^∞) for the reactions of 1- and 2-methylvinoxy radicals with O_2 obtained from the RRKM fitting are

$$k_3^\infty = (9.8 \pm 0.8) \times 10^{-13}\ \text{cm}^3\ \text{molecule}^{-1}\ \text{s}^{-1}$$

and

$$k_4^\infty = (1.3 \pm 0.1) \times 10^{-12}\ \text{cm}^3\ \text{molecule}^{-1}\ \text{s}^{-1}$$

respectively. The rate constant for reaction 3 fairly well agrees with the only one previous measurement (1.5×10^{-12} cm^3 molecule^{-1} s^{-1} at 760 Torr of SF_6).[21] The observed pressure dependence was also fitted to Troe and colleagues' formula[22] with the parameters (in cm^3−molecule−s units)

$$k_3^\infty = 9.8 \times 10^{-13},\ k_3^0 = 1.4 \times 10^{-29},$$
$$\text{and } F_{cent} = 0.487\ (\text{M} = \text{He},\ 15-333\ \text{Torr})$$

for reaction 3, and

$$k_4^\infty = 1.3 \times 10^{-12},\ k_2^0 = 3.7 \times 10^{-29},$$
$$\text{and } F_{cent} = 0.467\ (\text{M} = \text{He},\ 8-215\ \text{Torr})$$

for reaction 4.

In the fitting procedure, k^∞ was kept constant at the value derived by the RRKM calculation. However, to reproduce the experimental data, k^0 had to be changed significantly. Because the present experiments were done in a higher-pressure region, $[M] > [M]_c$, the results were not so sensitive to k^0. Further experimental investigations are needed for the limiting low-pressure rate constants.

The limiting high-pressure rate constants were determined with good accuracy by the RRKM calculation, although the derived E_0 bears less physical meaning because of the uncertainty of the transition-state model. The derived limiting high-pressure rate constants for reactions 3−5 are smaller than those for $C_2H_5 + O_2$, *n*- and *i*-$C_3H_7 + O_2$, and $CH_3CO + O_2$ (7.8, 8, 11, and 5.0×10^{-12} cm^3 molecule^{-1} s^{-1}, respectively).[23] This difference from the alkyl or acetyl radicals may be explained as follows: (1) The entrance part of the potential energy surface is distorted by the resonance stabilization so as to make the C−O separation at the transition state smaller, or (2) the transition state is *tight*, reflecting the tight structure of the resonantly stabilized radicals. The former possibility was also suggested by the fact that a saddle point was found along the B3LYP/6-31G(d) reaction coordinate.

The derived values of $\langle\Delta E_{down}\rangle$ (24−123 cm^{-1}) are in the allowable range for He buffer. By assuming the linear temperature dependence of $\langle\Delta E_{down}\rangle$,[24] the value for He buffer at 298 K is expected to be 40−150 cm^{-1} from the previous reports for C_2H_5,[24] *n*-C_3H_7,[25] *i*-C_3H_7,[26] *t*-C_4H_9O,[27] and CH_3O.[28] The large difference of $\langle\Delta E_{down}\rangle$ between reaction 3 (24 cm^{-1}) and reaction 4 (54 cm^{-1}) mainly resulted from the difference of the estimated ΔH, for which, however, no experimental or theoretical investigation has been reported. It should also be noted that, similar to k^0 described above, the present results are not so sensitive to $\langle\Delta E_{down}\rangle$ and the derived values are subject to change because of the uncertainty of the RRKM model.

The falloff pressure is apparently shifted to the higher-pressure side compared with the reactions of C_2H_5, *n*- and *i*-C_3H_7, and CH_3CO with O_2. In the case of the $C_2H_5 + O_2$ reaction, the rate constant is near the high-pressure limit at 10 Torr of He,[29] and in the case of *n*- and *i*-$C_3H_7 + O_2$ and $CH_3CO + O_2$, the rate constants are in the high-pressure limit at 1−4 Torr of He.[30,31] This could be explained by the resonance stabilization of the vinoxy radicals. As shown in Table 2, C−O bond dissociation energies (BDEs) of the peroxy radicals (112−121 kJ mol^{-1}) are smaller than those of alkylperoxy radicals (136−158 kJ mol^{-1}).[32] The smaller C−O BDEs can be attributed to the loss of the resonance stabilization energy when the C−O bond is formed. From the RRK or the RRKM theory, the higher shift of the falloff pressure is expected when the well becomes shallower, provided the molecular sizes are similar.

Conclusion

In the present study, the rate constants for the reactions of 1- and 2-methylvinoxy radicals with O_2 have been measured at room temperature (298 ± 5 K) and in the pressure range of 8−330 Torr (He buffer). Falloff pressure dependence was observed for both reactions, which indicates the dominance of recombination reactions forming peroxy radicals.

An RRKM analysis also supports the recombination mechanism and, from best fit to the experimental results, the limiting high-pressure rate constants were derived to be 9.8×10^{-13} for 1-methylvinoxy + O_2 and 1.3×10^{-12} cm^3 molecule^{-1} s^{-1} for 2-methylvinoxy + O_2. Methyl substitution at either 1- or 2-position was found to increase the limiting high-pressure rate constant. Compared with the alkyl radical reactions, the falloff range shifts toward higher pressure due to the shallower well caused by the resonance stabilization of vinoxy radicals. The smaller high-pressure limiting rate constant than the alkyl radical reaction may also be ascribed to the effect of resonance stabilization.

Supporting Information Available: Tables 1S−5S and Figure 1S containing information on the RRKM model based on the B3LYP/6-31G(d) level calculations (8 pages). This material is available free of charge via the Internet at http://pubs.acs.org.

References and Notes

(1) Inoue, G.; Akimoto, H. *J. Phys. Chem.* **1981, *74*, 425.**
(2) Gutman, D.; Nelson, H. H. *J. Phys. Chem*. **1983**, *87*, 3902.
(3) Lorenz, K.; Rhäsa, D.; Zellner, R.; Fritz, B. *Ber. Bensen-Ges. Phys. Chem.* **1985**, *89*, 341.
(4) Barnhard, K. I.; Santiago, A.; He, M.; Asmar, F.; Weiner, B. R. *Chem. Phys. Lett.* **1991**, *178*, 150.
(5) Zhu L.; Johnston, G. *J. Phys. Chem.* **1995**, *99*, 15114.
(6) Dimauro, L. F.; Heaven, M.; Miller, T. A. *J. Chem. Phys.* **1984**, *81*, 2339.
(7) Yamaguchi, M. *Chem. Phys. Lett.* **1994**, *221*, 531.
(8) Endo, Y.; Saito, S.; Hirota, E. *J. Chem. Phys.* **1985**, *83*, 2026.
(9) Washida, N.; Inomata, S.; Furubayashi, M. *J. Phys. Chem. A* **1998**, *102*, 7924.
(10) (a) Schmidt, V.; Zhu, G. Y.; Becker, K. H.; Fink, E. H. *Ber. Bunsen-Ges. Phys. Chem.* **1985**, *89*, 321; (b) Michael, J. V.; Nava, D. F.; Borkowski, R. P.; Payne, W. A.; Stief, L. J. *J. Chem. Phys.* **1980**, *73*, 6108.
(11) Williams, S.; Zingher, E.; Weisshaar, J. C. *J. Phys. Chem. A* **1998**, *102*, 2297.
(12) Quandt, R.; Min, Z.; Wang, X.; Bersohn, R. *J. Phys Chem. A* **1998**, *102*, 60.
(13) Koshi, M.; Nishida, N.; Murakami, Y.; Matsui, H. *J. Phys. Chem.* **1993**, *97*, 4473.
(14) Bofill, J. M.; Olivella, S.; Solé, A.; Anglada, J. M. *J. Am. Chem. Soc.* **1999**, *121*, 1337.
(15) Johnson, B. G.; Gill, P. M. W.; Pople, J. A. *J. Chem. Phys.* **1993**, *98*, 5612.
(16) Curtiss, L. A.; Raghavachari, K.; Trucks, G. W.; Pople, J. A. *J. Chem. Phys.* **1991**, *94*, 7221.
(17) Frisch, M. J.; Trucks, G. W.; Schlegel, H. B.; Scuseria, G. E.; Robb, M. A.; Cheeseman, J. R.; Zakrzewski, V. G.; Montgomery, J. A.; Stratmann, R. E.; Burant, J. C.; Dapprich, S.; Millam, J. M.; Daniels, A. D.; Kudin, K. N.; Strain, M. C.; Farkas, O.; Tomasi, J.; Barone, V.; Cossi, M.; Cammi, R.; Mennucci, B.; Pomelli, C.; Adamo, C.; Clifford, S.; Ochterski, J.; Petersson, G. A.; Ayala, P. Y.; Cui, Q.; Morokuma, K.; Malick, D. K.; Rabuck, A. D.; Raghavachari, K.; Foresman, J. B.; Cioslowski, J.; Ortiz, J. V.; Stefanov, B. B.; Liu, G.; Liashenko, A.; Piskorz, P.; Komaromi, I.; Gomperts, R.; Martin, R. L.; Fox, D. J.; Keith, T.; Al-Laham, M. A.; Peng, C. Y.; Nanayakkara, A.; Gonzalez, C.; Challacombe, M.; Gill, P. M. W.; Johnson, B. G.; Chen, W.; Wong, M. W.; Andres, J. L.; Head-Gordon, M.; Replogle E. S.; Pople, J. A. *Gaussian98 (Rev. A.5)*, Gaussian, Inc.: Pittsburgh, PA, 1998.
(18) Knyazev, V. D. *J. Phys. Chem. A* **1998**, *102*, 3916.
(19) Gilbert, R. G.; Smith, S. C. *Theory of Unimolecular and Recombination Reactions*; Blackwell: Oxford, 1990.
(20) Gilbert, R. G.; Smith, S. C.; Jordan, M. J. T. *UNIMOL Program Suite (Calculation of Falloff Curves for Unimolecular and Recombination Reactions)*, 1993. Available from the authors: School of Chemistry, Sydney University, NSW 2006, Australia or by e-mail to: gilbert_r@summer.chem.su.oz.au.
(21) Cox, R. A.; Munk, J.; Nielson, O. J.; Pagsberg, P.; Ratajczak, E. *Chem. Phys. Lett.* **1990**, *173*, 206.
(22) Gilbert, R. G.; Luther, K.; Troe, J. *Ber. Bunsen-Ges. Phys. Chem.* **1983**, *87*, 169.
(23) Atkinson, R.; Baulch, D. L.; Cox, R. A.; Hampson, R. F., Jr.; Kerr, J. A.; Rossi, M. J.; Troe, J. *J. Phys. Chem. Ref. Data* **1997**, *26*, 521.
(24) Feng, Y.; Niiranen, J. T.; Bencsura, Á.; Knyazev, V. D.; Gutman, D. *J. Phys. Chem.* **1993**, *97*, 871.
(25) Bencsura, Á.; Knyazev, V. D.; Xing, S.-B.; Slagle, I. R.; Gutman, D. *Proc. Symp. (Int.) Combust.* **1992**, *24*, 629.
(26) Seakins, P. W.; Robertson, S. H.; Pilling, M. J.; Slagle, I. R.; Gmurczek, G. W.; Bencsura, Á.; Gutman, D. Tsang, W. *J. Phys. Chem.* **1993**, *97*, 4450.
(27) Blitz, M.; Pilling, M. J.; Robertson, S. H.; Seakins, P. W. *Phys. Chem. Chem. Phys.* **1999**, *1*, 73.
(28) Oguchi, T.; Miyoshi, A.; Koshi, M.; Matsui, H. *Bull. Chem. Soc. Jpn.* **2000**, *73*, 53.
(29) Plumb, I. C.; Ryan, K. R. *Int. J. Chem. Kinet.* **1981**, *13*, 1011.
(30) Ruiz, R. P.; Bayes, K. D. *J. Phys. Chem.* **1984**, *88*, 2592.
(31) McDade, C. E.; Lenhardt, T. M.; Bayes, K. D. *J. Photochem.* **1982**, *20*, 1.
(32) Slagle, I. R.; Ratajczak, E.; Gutman, D. *J. Phys. Chem.* **1986**, *90*, 402.